WINCHESTER
A CITY IN THE MAKING

Archaeological excavations between 2002 – 2007
on the sites of Northgate House, Staple Gardens and the former Winchester Library, Jewry St

Section 19

Scientific dating and chronology

by Seren Griffiths, Alex Bayliss, Ben Ford, Mark Hounslow, Vassil Karloukovski, Christopher Bronk Ramsey, Gordon Cook and Peter Marshall

Section 19

Scientific dating and chronology

by Seren Griffiths, Alex Bayliss, Ben Ford, Mark Hounslow, Vassil Karloukovski, Christopher Bronk Ramsey, Gordon Cook and Peter Marshall

Introduction

Oxford Archaeology and Wessex Archaeology commissioned the University of Lancaster to sample 19 hearths from the Winchester Discovery Centre (Karloukovski and Hounslow 2006) and Northgate House (Karloukovski and Hounslow 2005) sites for archaeomagnetic dating during the excavation in 2004–6. Sixteen features could be dated using this technique.

In 2007 English Heritage agreed to fund the radiocarbon dating of 26 samples from contexts related to features dated to the Saxon period by the archaeomagnetic dates. This was a methodological study to verify independently the English archaeomagnetic calibration curve (Zananiri *et al.* 2007; Clark *et al.* 1988), by comparison with the radiocarbon dates and the excavated stratigraphic sequence using a Bayesian approach to chronological modelling (Buck *et al.* 1996). This methodological study is reported elsewhere (Hounslow *et al.* forthcoming). Following the preliminary modelling of this data, a further series of six radiocarbon samples were funded by Oxford Archaeology to ensure that the sample of the phase 4 deposits was representative, and thus enable these data to be analysed to address site-specific research objectives. Here, all the data are used to estimate the chronology of the site.

General approach

The Bayesian approach to the interpretation of archaeological chronologies has been described by Buck *et al* (1996). Bayesian models combine a range of archaeological information. Such models can include a number of chronological datasets: relative chronological information (often in the form of explicit stratigraphic relationships between sampled deposits), chronometric dating, and even information derived from historic sources or historically referenced material culture sources (such as coin evidence). Bayesian statistical analysis can result in more precise and reliable date estimates for events in the past through a formal modelling process. The '*posterior density estimates*' which are produced by Bayesian statistical models are, by convention, expressed *in italics*. This emphasises that, as with any model (Box 1979, 202), these date estimates are not absolute, they are interpretive expressions of the current state of knowledge. They can, and should be, subject to refinement as archaeological knowledge develops, and furthermore, they are only as reliable as the information on which they are based. Extreme rigour is thus essential in the evaluation of the data and beliefs that are included in the models.

The technique used here is a form of Markov Chain Monte Carlo sampling, which has been applied using the program OxCal v3.10 (Bronk Ramsey 1995; 1998; 2000; 2001). An OxCal model of the site's relative chronology is constructed based on the stratigraphic matrix. The program calculates the probability distributions of the individual calibrated radiocarbon results (Stuiver and Reimer 1993). It then attempts to reconcile these distributions with the relative ages of the samples, by repeatedly sampling each distribution (using the Metropolis-Hastings algorithm and the Gibbs sampler) to build up the set of solutions consistent with the model structure.

This process produces a posterior density estimate of each sample's calendar age, which occupies only part of the calibrated probability distribution (the prior distribution of the sample's calendar age). The posterior distribution is then compared to the prior distribution; an index of agreement is calculated that reflects the consistency of the two distributions. If the posterior distribution is situated in a high-probability region of the prior distribution, the index of agreement is high (sometimes 100% or more). If the index of agreement falls below 60% (a threshold value analogous to the 0.05 significance level in a χ^2 test), however, the radiocarbon result is regarded as inconsistent with the sample's calendar age, if the latter is consistent with the sample's age relative to the other dated samples. Sometimes this merely indicates that the radiocarbon result is a statistical outlier (more than 2 standard deviations from the sample's true radiocarbon age), but a very low index of agreement may mean that the sample is residual or intrusive (ie that its calendar age is different to that implied by its stratigraphic position).

An overall index of agreement is calculated from the individual agreement indices, providing a measure of the consistency between the archaeological phasing and the radiocarbon results. Again, this has a threshold value of 60%. The program is also able to calculate distributions for the dates of events that have not been dated directly, such as the beginning and end of a continuous phase of activity, and for the durations of phases of activity or hiatuses between such phases.

Objectives

The recovery of a large number of undisturbed *in situ* fired hearths throughout the Saxon sequence from the Northgate House site (NH) offered the potential to provide a precise chronology for the site, addressing a series of specific research questions:

- Did settlement on the site begin before the mid AD 880s (the date derived from Burghal Hidage for the foundation of the Alfredian burh)?
- How did the street pattern develop? Were the properties deliberately laid out at one time or did they spread organically from a central core?
- When did occupation of the Saxon properties on the site cease? Did it continue after AD 1066?
- Is it possible to refine the chronologies of the ceramics recovered from the sites?

The radiocarbon dating programme also contributes to these objectives, but was principally designed to test the accuracy of the existing archaeomagnetic calibration data for Britain (Clark *et al.* 1988). These dates would also provide additional calibration data for archaeomagnetic directions in this period during which it is poor replicated.

Sampling and laboratory processing

Archaeomagnetic sample selection

Archaeomagnetic samples were taken from suitable features which became accessible for sampling during the course of excavation. Sampling was undertaken by Vassil Karloukovski, Centre for Environmental Magnetism and Palaeomagnetism (CEMP), Lancaster University (Table 1). Between eight and ten oriented samples (monoliths) were collected from each hearth. Each monolith represented a 5 x 5 cm to 10 x 10 cm part of the hearth which was deemed suitable for sampling. This monolith was isolated by forming a groove around it, onto which a layer of plaster was then moulded onto the top surface. This plaster layer was made flat using a plastic plate. Onto this flat surface a reference direction was determined with respect to magnetic north (using a magnetic compass), and its dip direction was determined to an accuracy of ~1 degree.

Archaeomagnetic sample processing and quality assurance

Samples were consolidated at the laboratory in Lancaster as described by Jordanova *et al* (1996) and then sub-sampled. The direction and strength of the natural magnetization of the specimens from the hearth were measured at the CEMP (Lancaster University) using a Molspin fluxgate spinner magnetometer. The low-frequency magnetic susceptibility, χ_{LF}, was measured on a Bartington MS2 susceptibility meter. The natural remnant magnetisation (NRM) and χ_{LF} values were converted into volume-specific units. The NRM direction and χ_{LF} for all specimens from all the sampled hearths are listed in Karloukovski and Hounslow (2005). The Koenigsberger factor, Q_{NRM} was also determined from the NRM intensity and the χ_{LF} for each specimen. This ratio is an indication of the nature and the stability of the remnant magnetisation of the specimen (Karloukovski and Hounslow 2005).

Specimens from each hearth were demagnetised with alternating magnetic fields (AF) in seven to ten steps up to 50 mT, using a Molspin AF demagnetizer. The determination of the characteristic remnant magnetisation (ChRM) was based on the principal component analysis, using the program described by Kent *et al.* (1983).

Radiocarbon sample selection

During post-excavation assessment a chronological model was constructed of the existing archaeomagnetic dates, incorporating the relative dating provided by stratigraphy and the calendar dates provided by coins (*see* below). Single-entity (Ashmore 1999) short-life samples were selected for dating from contexts directly associated with the hearths which had provided the archaeomagnetic dates, and from contexts which were stratigraphically related to them. Wherever possible two samples were submitted from each context so that the potential for radiocarbon dates on residual material could be assessed. Material was selected which might have a functional relationship with the context from which was recovered (eg charcoal spreads directly overlying burnt hearths). The samples from NH4697 - silting on top of a Saxon street surface - were deliberately dated in knowledge that they would only provide *termini post quos* for overlying deposits.

Chronological modelling of these data was undertaken, which highlighted a bias in the sample of dates. Dates on samples from later deposits, in particular those from Phase 5 and 6, had poor agreement because the later part of the site's occupation had been truncated or was absent and so fewer features had been sampled for archaeomagnetic dating. For this reason, it was decided that the model should only attempt to estimate the chronology of the site during Phase 4, which has been divided into Phases 4.1 and 4.2. In order to ensure that the later part of this sequence was adequately sampled, six further samples were submitted for radiocarbon dating from contexts assigned to Phase 4.2 that could be related to the existing suite of dates by direct stratigraphic relationships. These included articulat*ing* animal bone from the same context, which were found to articulate during analysis, but which were not recorded as articulated at the point of excavation. These samples were probably articulated in the ground, or only slightly disturbed, and hence likely to be as close in age to their contexts as articulated bone.

Radiocarbon sample processing and quality assurance

Thirteen samples of charred plant remains were processed at the Oxford Radiocarbon Accelerator Unit using methods outlined in Hedges *et al.* (1989), and dated as described by Bronk Ramsey *et al.* (2004). Statistically consistent replicate measurements were made on one sample (<NH225> (NH3494) A; OxA-17181–2; T'=0.7; T'(5%)=3.8 ν=1; Ward and Wilson 1978).

Nineteen samples were dated by Accelerator Mass Spectrometry (AMS) at the Scottish Universities Environmental Research Centre (SUERC), East Kilbride in 2007-2008. The samples consisted of 16 carbonised cereal grains and pieces of charcoal and three animal bones. The charcoal and carbonised material were pretreated by the acid-base-acid protocol (Stenhouse and Baxter 1983) and the animal bone was prepared following a modified version of Longin (1971). Carbon dioxide was obtained from the pre-treated residues and bone samples by combustion in pre-cleaned sealed quartz tubes (Vandeputte *et al* 1996), converted to graphite (Slota *et al*.1987) and dated using methods outlined in Xu *et al.* (2004).

Both laboratories maintain continual programmes of quality assurance procedures, in addition to participation in international inter-comparisons (Scott 2003). These tests indicate no laboratory offsets and demonstrate the validity of the precision quoted. Identifications of the sampled material are presented in Table 2.

Results

Archaeomagnetic dating results

Hearth classification

All the hearths did not exhibit uniform preservation of archaeomagnetic directional data or magnetic behaviour. We have classified the hearths into three groups based on the directional scatter of their NRM to aid interpretation of the results. This classification also illustrates the differences in the material properties and magnetic preservation of the hearths.

- ***Class A**:* represented by hearths WOC (NH5188), WOF (NH4430), WOH (NH3484), WON (3680), and WOO (4733). The NRM directions in each of these hearths were tightly clustered and highly consistent between sister specimens (all specimens from a given sample). As a general rule, the hearths belonging to class A were those which consisted of homogeneous fine-grained, well burnt, hardened clay-rich layers.

- ***Class B***: represented by hearths WOD (NH2391), WOK (NH4523), WOM (NH4692), and WOP (NH3780). The material was again generally homogeneous, fine-grained and apparently well-baked. There was a good consistency between the NRM directions of sister specimens (ie from the same sample), but sometimes considerable directional deviation between the NRM directions of individual samples from each hearth. This directional deviation between the sample directions persists even after magnetic cleaning (*see* Karloukovski and Hounslow 2005 for the individual hearth results). This directional difference between samples from the same hearth indicates some internal disturbance within the hearth. Thus, class B hearths can be interpreted as materially like class A hearths but have experienced some fracturing (or other physical/magnetic disturbance) of their structure, since their last firing.

- ***Class C***: represented by hearths, WOA (NH2156), WOB (NH3177), WOE (NH4261), WOG (NH3462), WOI (NH7513, NH7522), WOJ (NH3506), and WOL (NH3576). These hearths possessed the most inhomogeneous material, sometimes of not well consolidated, coarser-grained (silty to sandy) material. Some of these hearths contained abundant flint, chalk, pottery or other fragments. Some of these hearths were not of uniform colour, possibly suggesting varying burning history for their different parts. The NRM directions of sister specimens for all samples (irrespective of which sample) were not particularly consistent, resulting in a scattering of data for the whole hearth. Hence, features belonging to this class of hearth required cutting many more specimens, to obtain a reliable estimate of the mean direction.

Archaeomagnetic calibration

The mean archaeomagnetic direction for each hearth was corrected for the local declination (−3.2^{o}) at Winchester for 2005 using the IGRF model (NASA-IGRF 2005). This was then converted via the pole method of Noel and Batt (1990) to the UK standard location at Meriden (φ=52.43^{o} N, λ=1.62^{o} W). This is necessary in order to compare the data to the British calibration data (Clark *et al* 1988). Calibrated dates were generated using the calibration curve proposed by Zananiri *et al* (2007). The results are given in Table 3. Probability densities of the calibrated dates were also generated using this curve (Fig. 1). These distributions were truncated at 400 BC and AD 1500 on the basis of prior archaeological knowledge. This was necessary because of the archaeomagnetic calibration curve folds back on itself at these dates, producing misleading bi-model distributions of calibrated dates. The probability densities provided by Lancaster University have been normalised and incorporated as part of the standardised likelihoods component of the Bayesian model described below.

Radiocarbon results

The results are given in Table 2, and are quoted in accordance with the international standard known as the Trondheim convention (Stuiver and Kra 1986). They are conventional radiocarbon ages (Stuiver and Polach 1977).

Radiocarbon calibration

The calibrations of these results, which relate the radiocarbon measurements directly to the calendrical time scale, are given in Table 2 and in Fig. 2. All have been calculated using the datasets published by Reimer *et al* (2004) and the computer program OxCal (v3.10) (Bronk Ramsey 1995; 1998; 2001). The calibrated date ranges cited are quoted in the form recommended by Mook (1986). The ranges in Table 2 have been calculated according to the maximum intercept method (Stuiver and Reimer 1986); all other ranges are derived from the probability method (Stuiver and Reimer 1993). Those ranges printed in italics in the text and tables are *posterior density estimates*, derived from the mathematical modeling described below.

Analysis and interpretation

A Bayesian chronological model consists of three fundamental components – the 'standardised likelihoods' and 'prior information' which are the inputs of the model, and the 'posterior beliefs' which are the output (Fig. 3). In this case, the probability distributions of calibrated archaeomagnetic and radiocarbon dates, and calendrical dates derived from coins, form the 'standardised likelihoods'. The 'prior information' consists of the relative dating provided by the stratigraphic sequence and our statistical assumption that activity on the site was continuous (see Bayliss 2007 and Bayliss *et al* 2007 for further discussion of building chronological models).

Scientific dating is available from four tenements, and four Saxon coins were recovered from the excavations, three of which can be associated with the properties.

Two archaeomagnetic dates are available from hearths in property BW6 (WOI1 and WOI2), and must date the use of this tenement. These deposits cannot be related by stratigraphy.

Scientific dates are available from three sequential deposits in property BW5 (Fig. 4). Two statistically consistent radiocarbon measurements are available from two oat grains dated from a layer of *in situ* burning (NH2391) (OxA-17137 and SUERC-13914; T'=1.2; T'(5%)=3.8; df=1), along with an archaeomagnetic date on the same feature (WOD NH2391). Later than this deposit are two statistically consistent results on fragments of short-life charcoal from a charcoal-rich layer (NH2424) within occupation deposits in the structure (OxA-17179 and SUERC-13915; T'=0.2; T'(5%)=3.8; ν=1). Later again is a hearth, dated by archaeomagnetism (WOA NH2156) and by two statistically inconsistent radiocarbon results on short-life charcoal from an *in situ* layer of burning within the hearth (OxA-17174 and SUERC-13908; T'=6.3; T'=3.8; ν=1). Because of this inconsistency, the earlier of these two charcoal fragments has been interpreted as redeposited and therefore incorporated into the Bayesian model only as a *terminus post quem* for the end of the use of this phase of activity in the property.

Scientific dates are available from six sequential deposits in property BW4 (Fig. 5). Two statistically consistent radiocarbon determinations on short-life charcoal fragments are available from an occupation horizon (NH3587) (OxA-17173 and SUERC-13907; T'=0.3; T'(5%)=3.8; ν=1). These dates are earlier than a hearth, which has been dated by archaeomagnetism (WOL(NH3576)). Later again are two statistically inconsistent radiocarbon results on short-life material from a lens of charcoal associated with firing hearth

(NH3578)(OxA-17172 and SUERC-13906; T'=6.9; T'(5%)=3.8; ν=1). Again, because of the inconsistency in the radiocarbon results, the earlier of the two charcoal fragments has been interpreted as redeposited and has only been used as a *terminus post quem* for overlying deposits. Later than this is another hearth dated by archaeomagnetism (WOJ(NH3506)). Two statistically consistent measurements on fragments of short-life charcoal from fuel associated with the firing of this hearth (NH3494) (SUERC-13917 and OxA-17181–2; T'=1.4; T'(5%)=3.8; ν=1) are also available. Later than this, are two statistically consistent radiocarbon measurements on charred plant remains from occupation horizon (NH3260) (SUERC-19280 and SUERC-19284; T'=0.7; T'(5%)=3.8; ν=1). A silver penny of Edgar or Alfred from underlying context (NH3466; SF223) provides a *terminus post quem* of AD 871–975 for occupation layer (NH3260). Two statistically inconsistent radiocarbon results (SUERC-19285 and SUERC-19286; T'=5.0; T'(5%)=3.8; ν=1), however, have been obtained from another occupation horizon (NH3175), which is stratigraphically later than (NH3260). The earlier of these, SUERC-19285 on a grain of wheat, has been interpreted as residual and has been included in the model only as a *terminus post quem* for the end of the use of property BW4.

Scientific dates are available from three stratigraphic strings in property BW3 (Fig. 6). A hearth which has been dated by archaeomagnetism (WON(NH3680)) is earlier than two statistically inconsistent radiocarbon results on short-life charcoal fragments from a layer of *in situ* burning within the property (NH3664) (OxA-17178 and SUERC-13910; T'=4.4; T'(5%)=3.8; ν=1). Because of the inconsistency in these radiocarbon results, the earlier of the two charcoal fragments has been interpreted as redeposited and has only been used as a *terminus post quem* for overlying deposits. Also later than hearth (WON(NH3680)) is another hearth dated by archaeomagnetism (WOB(NH3177)). A layer of burning within this hearth produced a short-life charcoal fragment which must be intrusive as it dates to the fifteenth century cal AD (OxA-17175). Hearth (WOB(NH3177)) dates to AD 1117-1229 (95% confidence), which is consistent with the associated Phase 6 pottery assemblage. It has been included in the model as a *terminus ante quem* for the end of Phase 4.

The second sequence of dated deposit in property BW3 cannot be related to the sequence just described, and contains a series of deposits in Phase 5. For this reason they have only been included in the model as *termini ante quos* for the end of Phase 4. All are comfortably later than hearth (NH4692) in property BW2 (see below), which is stratigraphically earlier than (NH4458), a discrete rake-out from oven (NH4485). This produced two statistically inconsistent radiocarbon measurements on cereal grains (OxA-17180 and SUERC-13916; T'=6.7; T'(5%)=3.8; ν=1). The earlier of these (OxA-17180) has only been included in the model as a *terminus post quem* for the overlying hearth, which has been dated by archaeomagnetism (WOF(NH4430)). Later than this hearth are two statistically inconsistent radiocarbon measurements on short-life material from an occupation layer (NH4373)(OxA-17176 and SUERC-13904; T'=8.7; T'(5%)=3.8; ν=1). The earlier of these may therefore be residual and has only been included in the model as a *terminus post quem* for the end of occupation of property BW2.

Hearth WOH(NH3484) has been dated by archaeomagnetism to AD 1195-1267 (95% confidence). This Phase 5 feature is recorded as being stratigraphically earlier than (NH4458) and the rest of the sequence just described. The scientific dates are in poor agreement with this interpretation, as both the archaeomagnetic date from Hearth WOF(NH4430) and the radiocarbon dates from (NH4458) and (NH4373) are earlier than the archaeomagnetic date from WOH(NH3484). Both archaeomagnetic dates in this sequence are Class A and so it is unlikely that either is inaccurate. In these circumstances, it appears that the stratigraphic record may be in error. Examination of the sequence of stratigraphic relationships between (NH3484) and (NH4458) suggests that it may be the relationship of unplanned occupation horizon (NH3486) with floor (NH3667) which has been misinterpreted. This relationship was inferred over a horizontal distance of more than 4m in an area of heavy slumping, and it appears that similar charcoal rich occupation horizons may have been conflated. For this reason, we suggest that WOH(NH3484) is not related stratigraphically to the other dated deposits from property BW3, and so it has been included in the model simply as a *terminus ante quem* for the end of Phase 4.

Dates are available from 12 deposits that can be stratigraphically related in property BW2 (Fig. 7). From the base of the sequence, an archaeomagnetic date has been produced on hearth WOO NH4733. This feature is earlier than hearth (NH4692), which has also been dated by archaeomagnetism (WOM NH4692). Two statistically consistent determinations on short-life charcoal from the silting of the Saxon street surface (NH4697) (OxA-17177 and SUERC-13909; T'=0.9; T'(5%)=3.8; ν=1) provide *termini post quem* for hearth (WOM NH4692). The uncertain taphonomy of the dated material means that we have not interpreted these dates as later than hearth (NH4733), even though the street surface itself sealed this hearth (see Fig. 7).

Two stratigraphic sequences are later than hearth (NH4692). The first sequence begins with two statistically consistent radiocarbon measurements on charred hazelnut shell from a discrete charcoal-rich deposit (NH4580) associated with *in situ* burning of burnt surface (NH4557)(OxA-17183 and SUERC-13918; T'=1.7; T'(5%)=3.8; ν=1). Later than deposit (NH4580) is hearth (NH4523), which has produced an archaeomagnetic date (WOK NH4523). This produced an anomalously late archaeomagnetic date, both in relation to the stratigraphic sequence and the associated ceramic assemblage. There is evidence in this hearth of possible disturbance, since four of the nine samples show consistent within-sample deviation from the remaining five samples which have tightly grouped specimen directions. It has therefore been excluded from the model. Above this was a charcoal spread within an occupation horizon (NH4507), which produced a single radiocarbon age on a charred oat grain (SUERC-13920). In turn, this is earlier than hearth (NH4261), dated by an archaeomagnetic date (WOE NH4261) and two statistically consistent radiocarbon determinations on short-life charcoal from a discrete charcoal spread (NH4394) associated with *in situ* burning from the hearth (OxA-17184 and SUERC-13919; T'=2.1; T'(5%)=3.8; ν=1). Later than this are two statistically consistent radiocarbon measurements on animal bone from occupation deposit (NH4379)(SUERC-19287–8; T'=2.7; T'(5%)=3.8; ν=1). One of these samples, SUERC-19288, was a cattle carpal which was recovered in articulation with a radius. This sample, at least, cannot be residual. The second sequence contains a series of Phase 5 deposits in property BW3, as hearth WOM(NH4692) is stratigraphically earlier than rake-out (NH4458). The sequence above this has been described above (see Fig. 6).

Pit (NH4095) cannot be stratigraphically related to the deposits from property BW2 that have produced scientific dates. It produced a silver penny of Athelstan (AD 924–939) and an Anglo-Saxon sceat, tentatively assigned to series K and thus probably minted between *c.* AD 720 and AD 740, however, which provide *termini post quem* for the end of the use of property BW2.

Archaeological interpretation: the site chronology

The overall structure of the chronological model which incorporates this interpretation of the archaeological data as prior information is shown in Fig. 8. This treats the phase of activity represented by Phase 4 as a continuous, and relatively constant period of occupation. Although in reality the tenements probably continued in use beyond this pottery phase, these deposits frequently have not survived later truncation and had been under-sampled by both the excavation and the dating programme. For this reason, it was decided that a chronological model of this period of use of the site alone was more realistic than that for the full span of the use of the properties. The component section of this model relating to property BW6 is shown in Fig. 9. Elements relating to properties BW5, BW4, BW3 and BW2 are shown in Figs 10-12, and 13 respectively. The large square brackets down the left hand side of these figures along with the OxCal chronological command language define the model exactly.

This model has good overall agreement ($A_{overall}$=80.7%, A'c=60.0%; Bronk Ramsey 1995: 429), and suggests that the Saxon occupation of these tenements began in *cal AD 810-890 (88% probability; start Saxon*; Fig. 8*)* or *cal AD 910-940 (7% probability)* and probably *cal AD 840-890 (68% probability*). It is *86.3% probable* that these tenements were established before the 880s AD, which according to the Burghal Hidage is regarded as the foundation date of the Alfredian burh.

It is also probable that these properties and the associated street pattern were established after the Viking raid of Hamwic documented in AD 842 (*87.1% probable*). It is not possible to establish whether these properties were established before or after the documented Viking raid of Winchester in AD 860 (the probability that they existed before AD 860 is *41.1%*, or only after AD 860 is *58.9%*).

Properties BW2, BW4 and BW5 appear to have been established in the second half of the 9th century AD (Fig. 14), it is possible that properties BW3 and BW6 were established slightly later, in the first half of the 10th century AD. However, properties BW3 and BW6 are more poorly dated for their earlier parts of their sequences than the other properties. The establishment of properties BW2, 4 and 5 might therefore have formed part of a planned development, and it is possible that the other two properties were also established as part of this initial phase. It is possible that the properties could have been built up over a few decades rather than all being established at exactly the same time. Either way, it is likely that the first inhabitants of each tenement knew each other, and that occupation in this place, at this time, was directly related to the development of *Brudenstrete*.

Archaeological interpretation: the ceramic chronologies

The site matrix provides the primary means of presenting change through time derived from stratigraphic relationships. Further to this, ceramic typologies provide means of exploring change through time at the site. Four pottery site phases were established at Winchester Northgate House, which have relevance for Saxon chronometric results. The pottery phases were generated from the assemblages recovered from the site, and estimates for them are shown in Table 4. The end of phase 4.1 and start of phase 4.2 is defined by the appearance of Late Saxon flinty wares. These include MAV, the probably local chalk temper ware, with some flint. Also present in 4.2 are the more diagnostic Michelmersh-Type Ware and Winchester Ware. The end of phase 4.2 and the start of phase 5 is defined by a number of wares, most diagnostic of which is the Tripod Pitcher Ware, but also represented by Newbury/Kennet Valley Fabric B, coarse grey sandy ware (MOE), sandy ware with flint and chalk (MBK), and sandy ware with flint, chalk and 'organic' temper (MAF). In actuality, the calendar dates of these pottery chronologies are relatively poorly understood, with considerable variability in the dating of individual wares, and especial reliance placed on rare, finewares (Cotter pers. comm.). The archaeomagnetic and radiocarbon data, provide independent means of estimating the calendar dates for these phases as described below.

The model shown in Fig.15 is based on the assumption that the ceramic phases 4.1, 4.2 and 5 are abutting (Buck *et al*. 1992; Naylor and Smith 1988), with the estimated dates of the samples derived from the model shown in Fig. 8. From this the dates of four unknown archaeological *"events"*, the beginning of ceramic phase 4.1, the end of ceramic phase 4.1, start of ceramic phase 4.2, etc can be derived as estimates of the dates of transition from one phase to another. The model has good overall agreement ($A_{overall}$=114.3%, A'c=60.0%); estimates for the dates of ceramic phases are given in Table 4, and in Fig. 16.

Sensitivity analysis

Sensitivity analyses are alternative interpretive models constructed from alternative ways of modelling the information previously presented. By comparing different analyses it is possible to investigate the extent to which the answers are dependent on the radiocarbon measurements, and the stratigraphic sequence. The format of the model is identical to shown in Fig. 15, but this time the radiocarbon and archaeomagentic dates have not been derived from the model shown in Fig. 8. This has been undertaken to explore how much the results are influenced by the stratigraphic relationship between samples. The model has good overall agreement ($A_{overall}$=109.4%, A'c=60.0%); estimates for the dates of ceramic phases are given in Table 4, and in Fig. 17. The results suggest that the use of prior estimates derived from the stratigraphic relationships between samples in Fig. 8 included in the model shown in Fig. 15 does not strongly affect the outputs of the model.

References

Ashmore, P, 1999 Radiocarbon dating: avoiding errors by avoiding mixed samples, *Antiquity*, **73**, 124–30

Bayliss, A, Bronk Ramsey, C, van der Plicht, J, and Whittle, A, 2007 Bradshaw and Bayes: towards a timetable for the Neolithic, *Cambridge Archaeol J*, **17(1) suppl**, 1–28

Bayliss, A, 2007 Bayesian buildings: an introduction for the numerically challenged, *Vernacular Architect*, **38**, 76–87

Box, G. E. P, 1979 Robustness in scientific model building, in *Robustness in Statistics,* eds. R L Launer and G N Wilkinson, New York: Academic Press, 201-36.

Bronk Ramsey, C, 1995 Radiocarbon calibration and analysis of stratigraphy: the OxCal program, *Radiocarbon*, **36**, 425–30

Bronk Ramsey, C, 1998 Probability and dating, *Radiocarbon*, **40**, 461–74

Bronk Ramsey, C. 2000 Comment on "The use of Bayesian statistics for ^{14}C dates of chronologically ordered samples: a critical analysis". *Radiocarbon* **42**, 199–202.

Bronk Ramsey, C, 2001 Development of the radiocarbon calibration program OxCal, *Radiocarbon*, **43**, 355–63

Bronk Ramsey, C, Higham, T, and Leach, P, 2004 Towards high precision AMS: progress and limitations, *Radiocarbon*, **46**, 17–24

Buck, C E, Litton, C D, and Smith, A F M, 1992 Calibration of radiocarbon results pertaining to related archaeological events, *J Archaeol Sci*, **19**, 497–512

Buck, C E, Cavanagh, W G, and Litton, C D, 1996 *Bayesian Approach to Interpreting Archaeological Data*, Chichester

Clark, A J, Tarling, D J, and Noël, M, 1988 Developments in archaeomagnetic dating in Britain, *J Archaeol Sci*, **15**, 645–67

Hedges, R E M, Bronk, C R and Housley, R A 1989 The Oxford Accelerator Mass Spectrometry facility: technical developments in routine dating, *Archaeometry*, **31**, 99–113

Jordanova N, Jordanova J. and Karloukovski, V, 1996, Magnetic fabric of Bulgarian loess sediments derived by using various sampling techniques, *Studia geophyisca et geodetica.,* **40**, 36-49.

Karloukovski, V, and Hounslow, M. W, 2005 Report on the archaeomagnetic dating of seventeen hearths from Northgate, Winchester

Karloukovski, V, and Hounslow, M. W, 2006 Report on the archaeomagnetic dating of two Roman hearths from Jewry Street, Winchester

Kent, J T, Briden, J C, and Mardia, K V, 1983. Linear and planar structure in ordered mulivariate data as applied to progressive demagnetisation of palaeomagnetic remanence. *Geophys. Jour. Royal. astro. Soc*., **81**, 75-87.

Longin, R, 1971 New method of collagen extraction for radiocarbon dating, *Nature*, **230**, 241–2

Mook, W G, 1986 Business meeting: Recommendations/Resolutions adopted by the Twelfth International Radiocarbon Conference, *Radiocarbon*, **28**, 799

NASA-IGRF Geomagnetic Field Model, 2005 http://nssdc.gsfc.nasa.gov/space/model/models/igrf.html

Naylor, J C, and Smith, A F M, 1988 An archaeological inference problem, *Journal of the American Statistical Association* **83**, 588–595

Noel M, and Batt C M, 1990, A method for correcting geographically separated remanence directions for the purpose of archaeomagnetic dating, *Geophys. J. Int.*, **102**, 753-756,

Reimer, P J, Baillie, M G L, Bard, E, Bayliss, A, Beck, J W, Bertrand, C J H, Blackwell, P G, Buck, C E, Burr, G S, Cutler, K B, Damon, P E, Edwards, R L, Fairbanks, R G, Friedrich, M, Guilderson, T P, Hogg, A G, Hughen, K A, Kromer, B, McCormac, F G, Manning, S, Bronk Ramsey, C, Reimer, R W, Remmele, S, Southon, J R, Stuiver, M, Talamo, S, Taylor, F W, van der Plicht, J, and Weyhenmeyer, C E 2004 IntCal04 Terrestrial Radiocarbon Age Calibration, 0–26 cal kyr BP, *Radiocarbon*, **46**, 1029–58

Scott, E M (ed), 2003 The Third International Radiocarbon Intercomparison (TIRI) and the Fourth International Radiocarbon Intercomparison (FIRI) 1990–2002: results, analysis, and conclusions, *Radiocarbon*, **45**, 135−408

Slota Jr, P J, Jull, A J T, Linick, T W and Toolin, L J, 1987 Preparation of small samples for ^{14}C accelerator targets by catalytic reduction of CO, *Radiocarbon*, **29**, 303–6

Stenhouse, M J, and Baxter, M S, 1983 ^{14}C dating reproducibility: evidence from routine dating of archaeological samples, *PACT*, **8**, 147–61

Stuiver, M, and Kra, R S, 1986 Editorial comment, *Radiocarbon*, **28(2B)**, ii

Stuiver, M, and Polach, H A, 1977 Reporting of ^{14}C data, *Radiocarbon*, **19**, 355–63

Stuiver, M, and Reimer, P J, 1986 A computer program for radiocarbon age calculation, *Radiocarbon*, **28**, 1022–30

Stuiver, M, and Reimer, P J, 1993 Extended ^{14}C data base and revised CALIB 3.0 ^{14}C age calibration program, *Radiocarbon*, **35**, 215–30

Vandeputte, K, Moens, L, Dams, R, 1996 Improved sealed-tube combustion of organic samples to CO_2 for stable isotopic analysis, radiocarbon dating and percent carbon determinations, *Analytical Letters*, **29**, 2761–73

Ward, G K, and Wilson, S R, 1978 Procedures for comparing and combining radiocarbon age determinations: a critique, *Archaeometry*, **20**, 19-31

Xu, S, Anderson, R, Bryant, C, Cook, G T, Dougans, A, Freeman, S, Naysmith, P, Schnabel, C, and Scott, E M, 2004 Capabilities of the new SUERC 5MV AMS facility for ^{14}C dating, *Radiocarbon*, **46**, 59–64

Zananiri, I, Batt, C M, Tarling, D, Lanos, P, and Linford, P, 2007 Archaeomagnetic secular variation in the UK during the past 4000 years and its application to archaeomagnetic dating, *Physics of the Earth and Planetary Interiors,* **160**, 97–107

Section 19 Figures and Tables

Figure 1: Saxon archaeomagnetic dates from Northgate House, Winchester, calibrated by the probability method (Stuiver and Reimer 1993) using the calibration curve of Zananiri *et al* (2007); distributions have been truncated on the basis of archaeological information to exclude possible dates before 400 BC or after AD 1500.

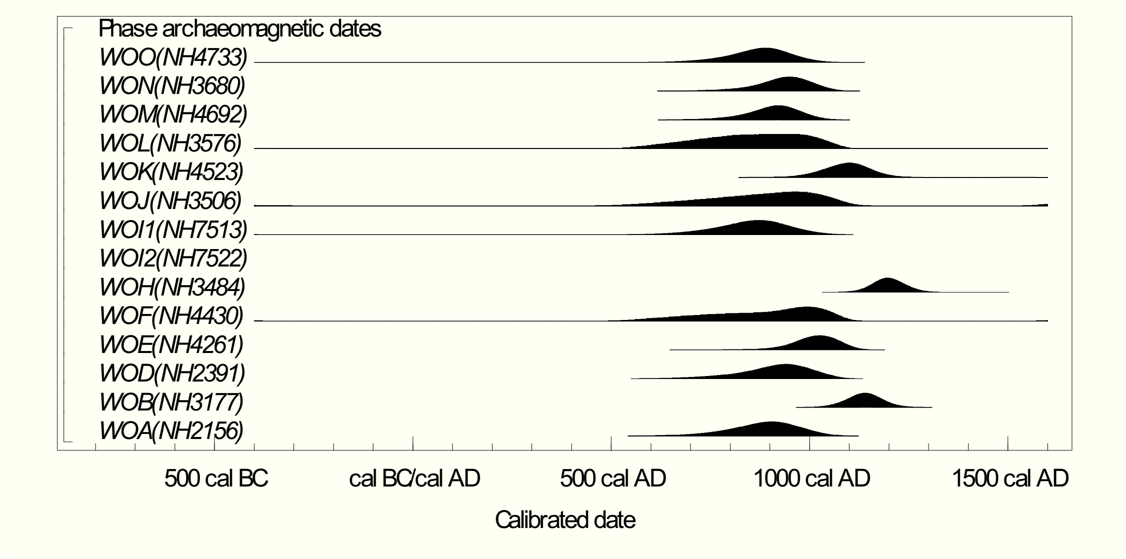

Figure 2: Radiocarbon dates from Northgate House, Winchester, calibrated by the probability method (Stuiver and Reimer 1993) using the calibration curve of Reimer *et al* (2004).

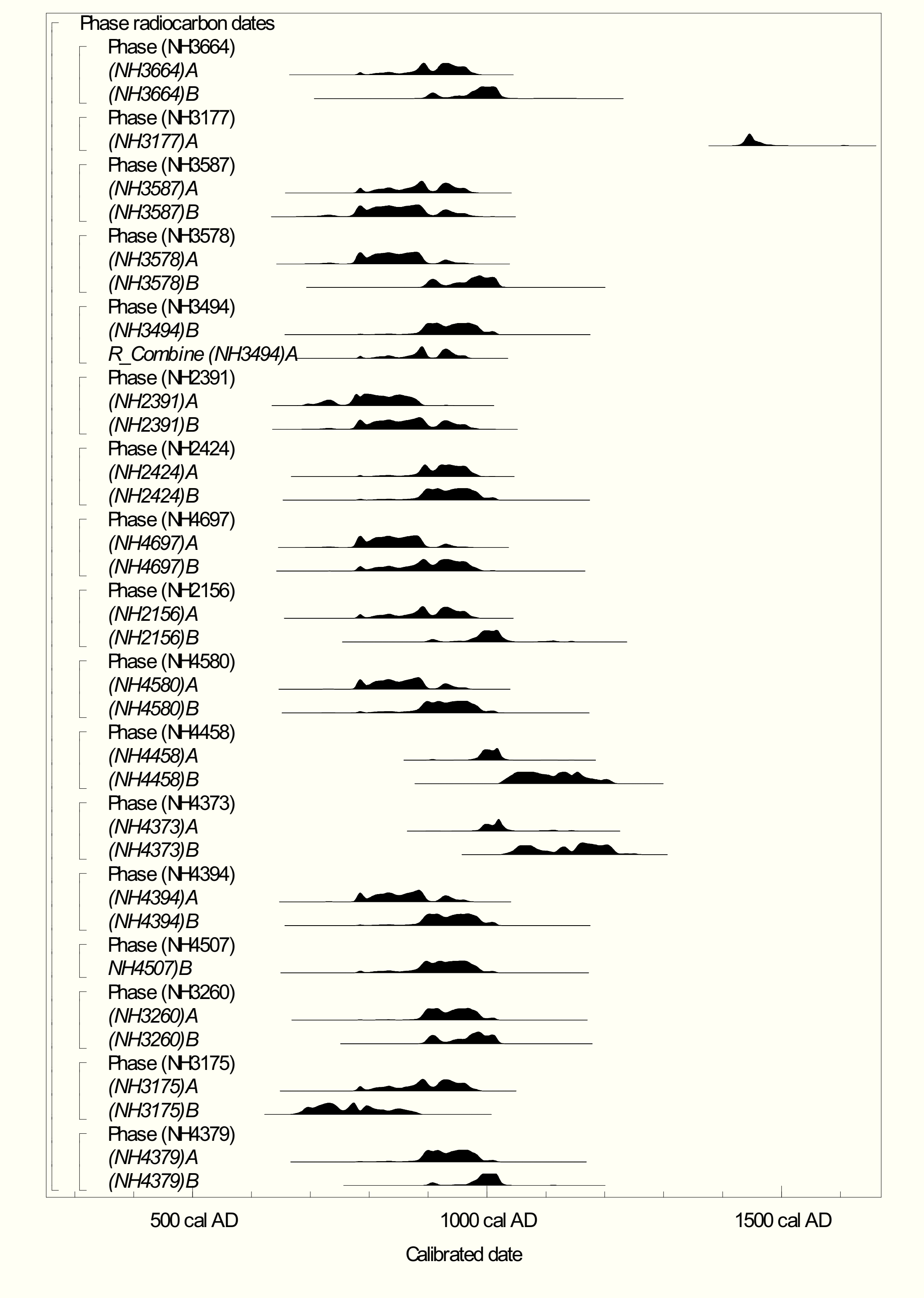

Figure 3: Components of a Bayesian chronological model

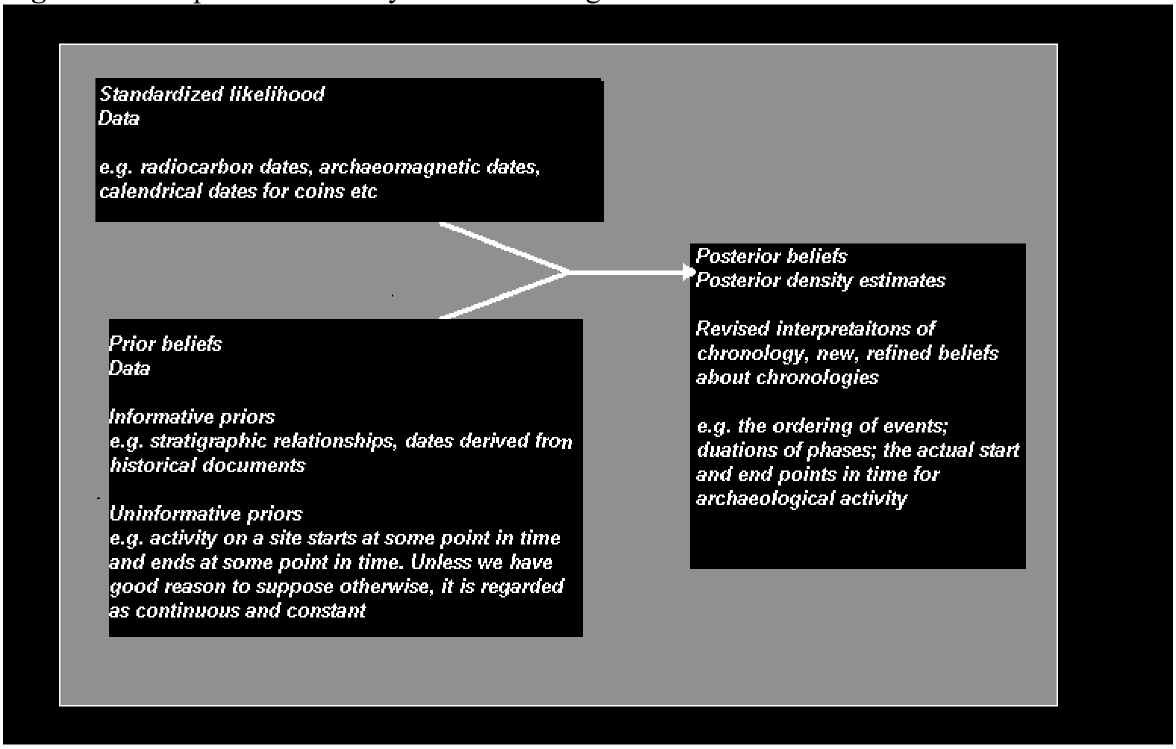

Figure 4: Summary of the relationships between dated deposits in property BW5

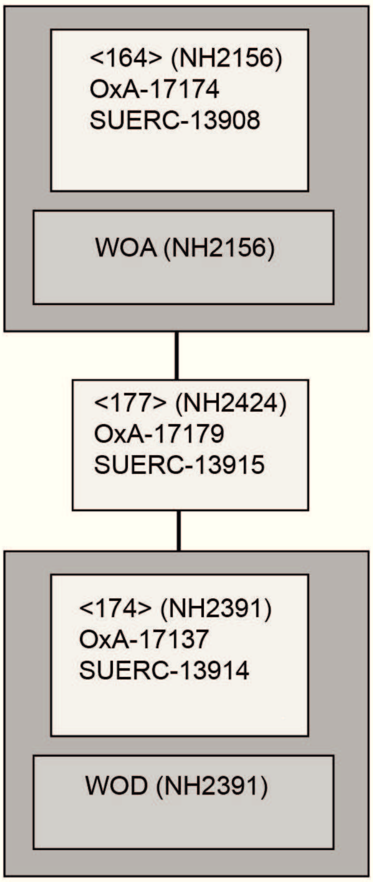

Figure 5: Summary of the relationships between dated deposits in property BW4

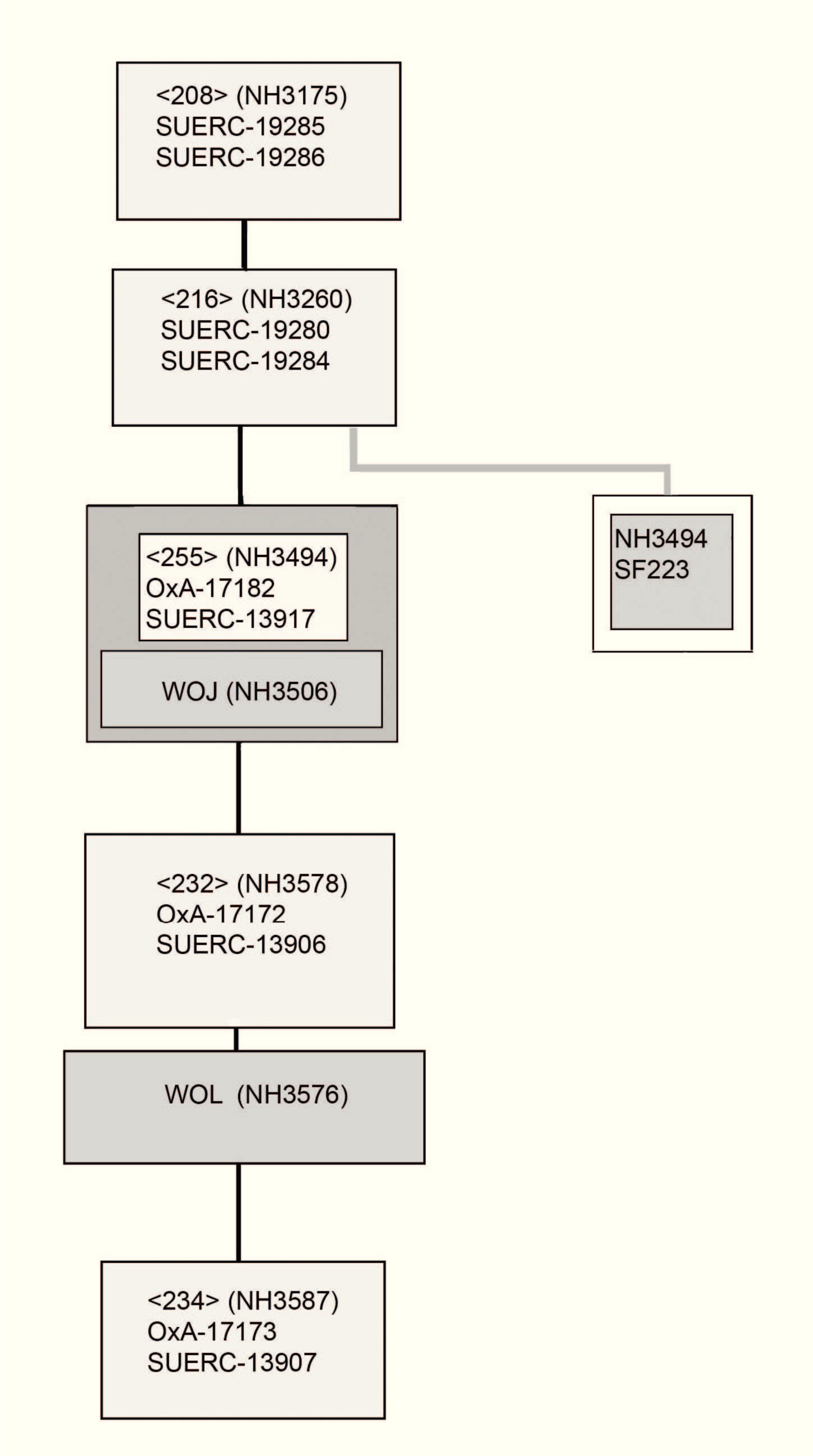

Figure 6: Summary of the relationships between other dated deposits in property BW3, (NH4458) is stratigraphically later than hearth (NH4692) in property BW2 (see Fig. 7)

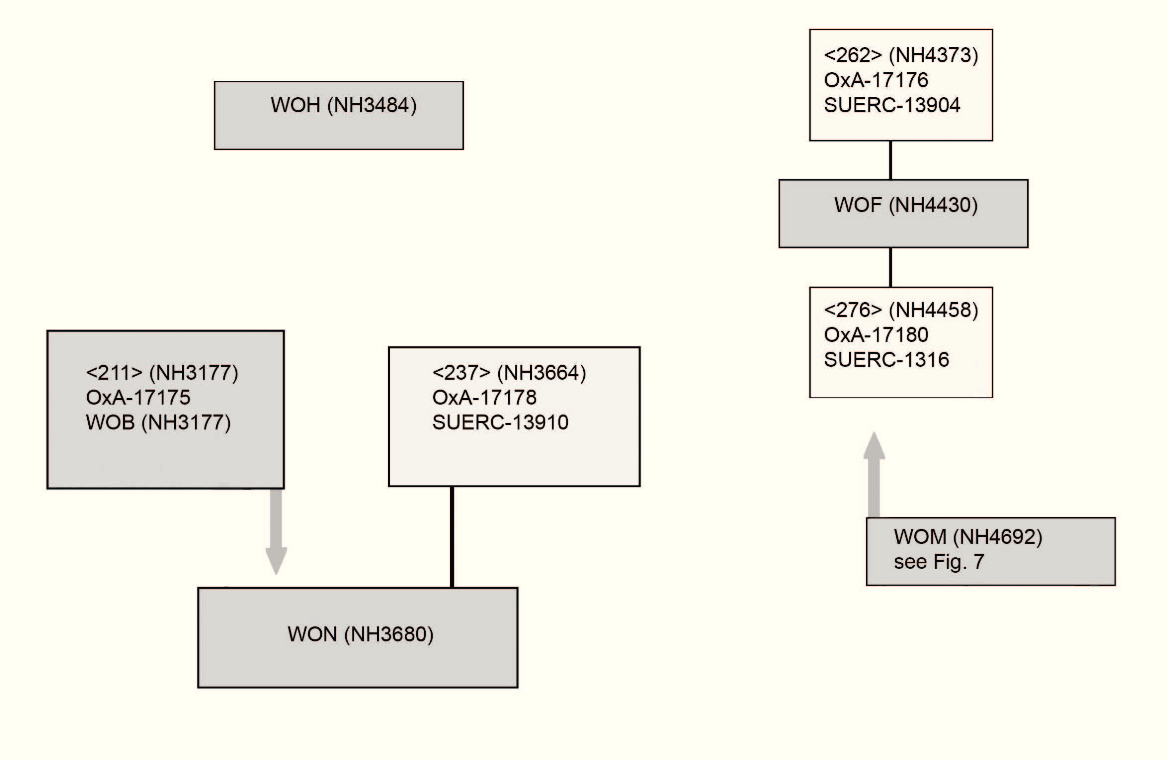

Figure 7: Summary of the relationships between dated deposits in property BW2, hearth (NH4692) is stratigraphically earlier than (NH4458) in property BW3 (see Fig. 6)

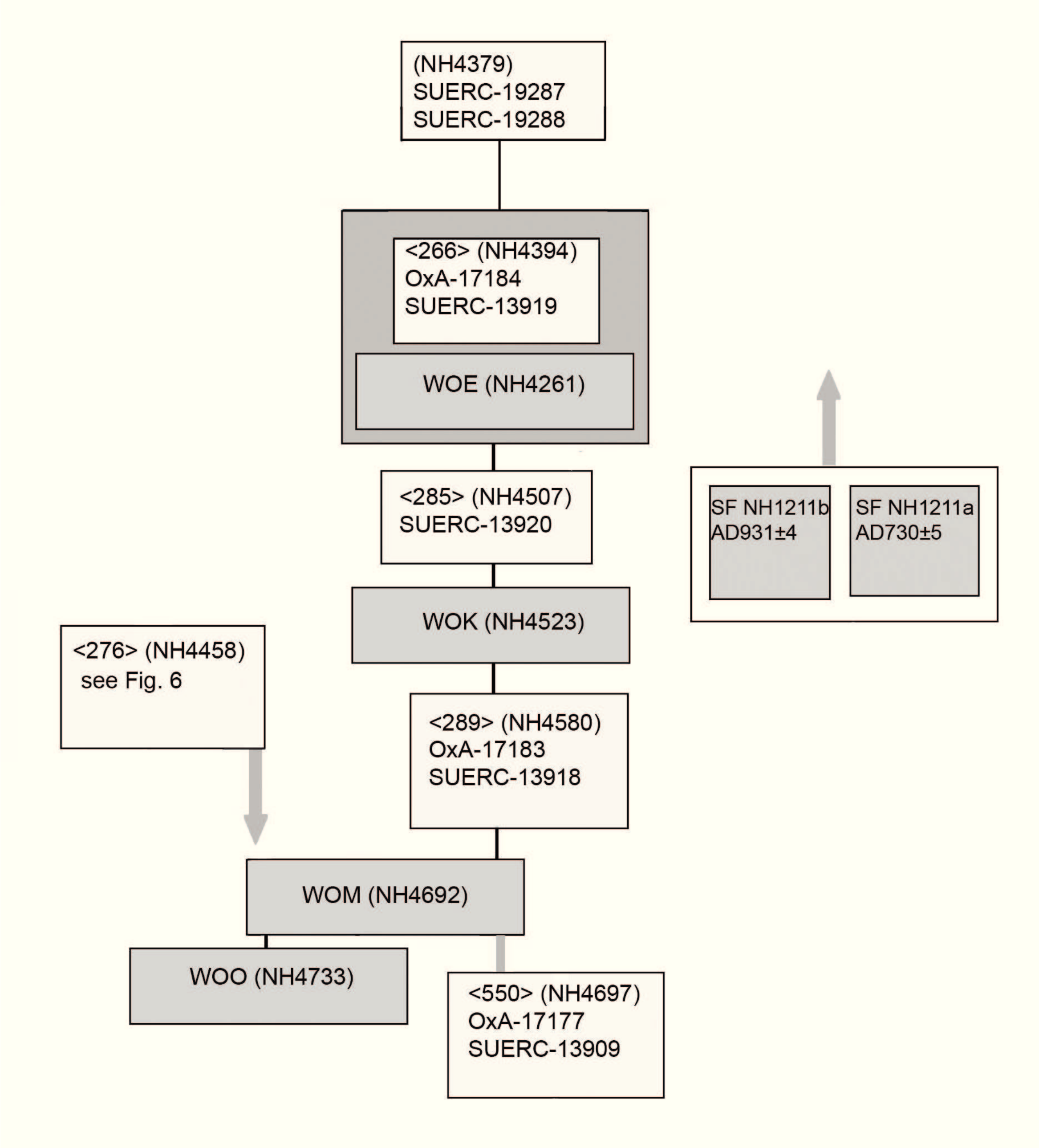

Figure 8: Overall structure for the chronological model of phase 4 deposits from Northgate House, Winchester. The component sections of this model are shown in detail in **Figures 9-12**. The distributions correspond to aspects of the model. For example, the distribution '*start Saxon*' is the estimated date when activity on the site began. The large square brackets down the left hand side of these figures along with the OxCal keywords define the overall model exactly.

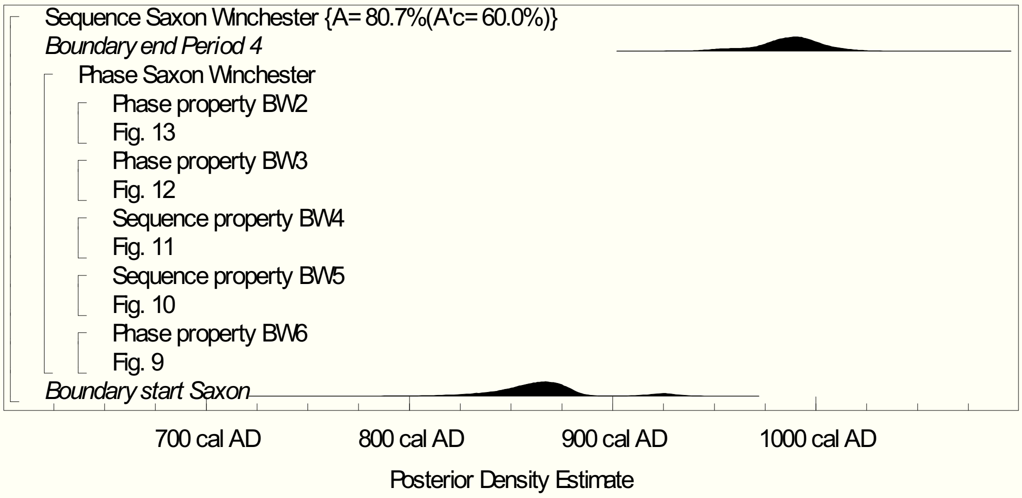

Figure 9: Probability distributions of dates from property BW6 at Northgate House, Winchester. Each distribution represents the relative probability that an event occurred at a particular time. For each of the dates two distributions have been plotted, one in outline, which is the result produced by the scientific evidence alone, and a solid one, which is based on the chronological model used. The 'event' associated with, for example, '*WOI17513Batt*', is the last firing of hearth (NH7513). Dates followed by a question mark have been calibrated (Stuiver and Reimer 1993), but not included in the chronological model for reasons explained in the text. The large square brackets down the left hand side of **Figures 8–12** along with the OxCal keywords define the overall model exactly.

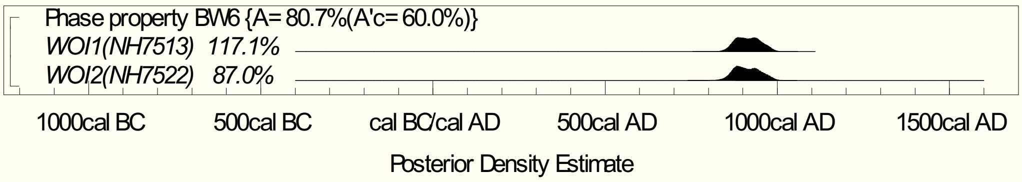

Figure 10: Probability distributions of dates from property BW5 at Northgate House, Winchester. The format is identical to that of **Figure 9**. The large square brackets down the left hand side of **Figures 8–12** along with the OxCal keywords define the overall model exactly.

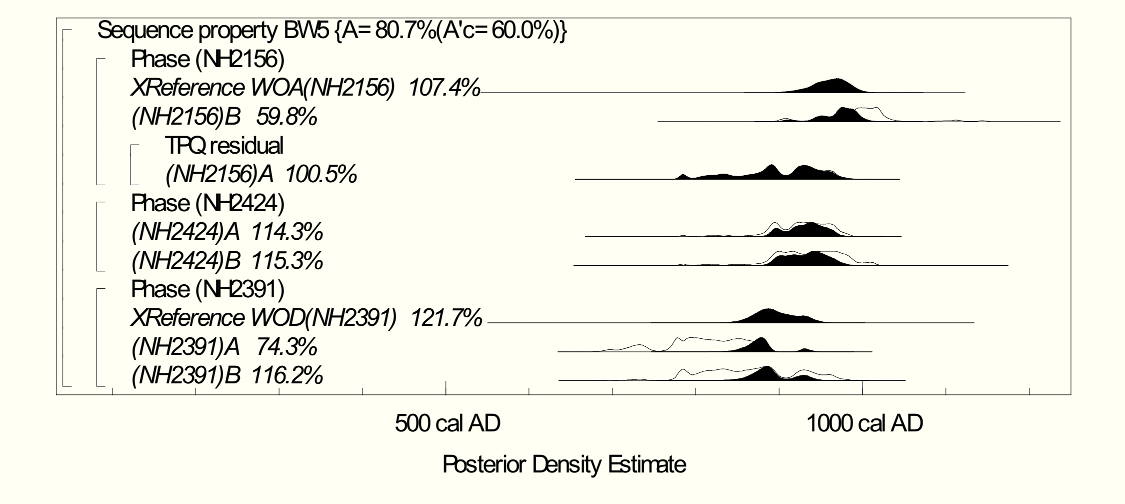

Figure 11: Probability distributions of dates from property BW4 at Northgate House, Winchester. The format is identical to that of **Figure 9**. The large square brackets down the left hand side of **Figures 8–12** along with the OxCal keywords define the overall model exactly.

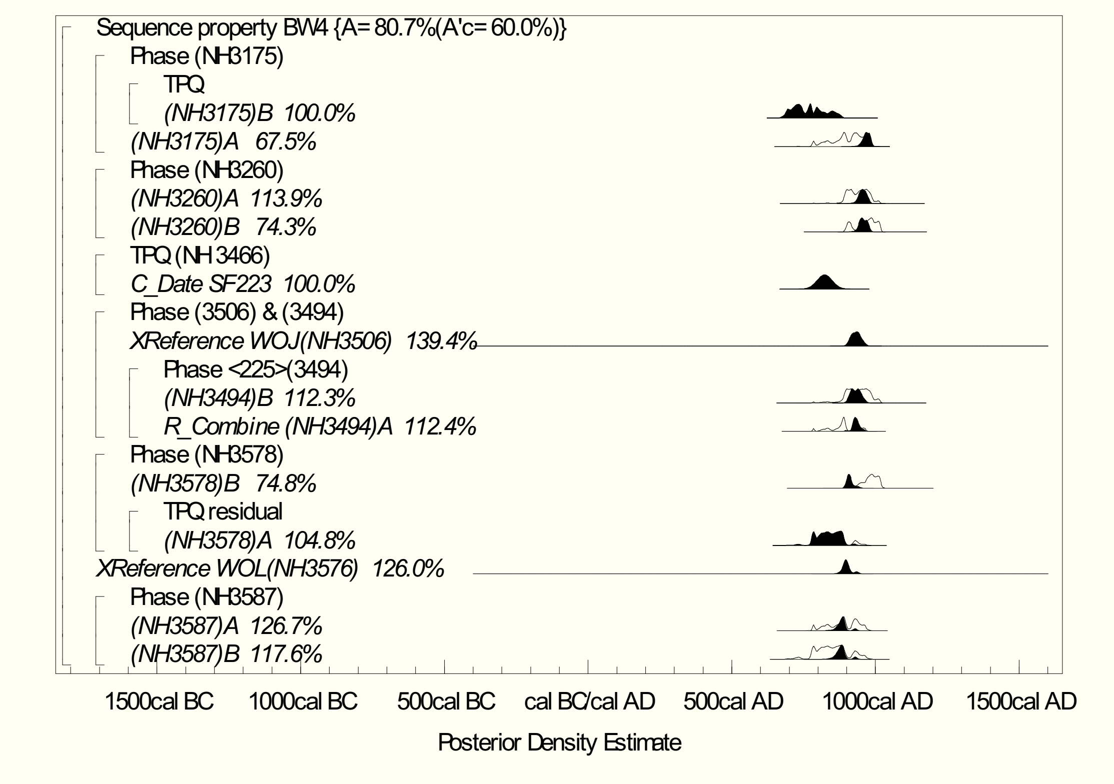

Figure 12: Probability distributions of dates from property BW3 at Northgate House, Winchester. The format is identical to that of **Figure 9**. The large square brackets down the left hand side of **Figures 8**–**12** along with the OxCal keywords define the overall model exactly.

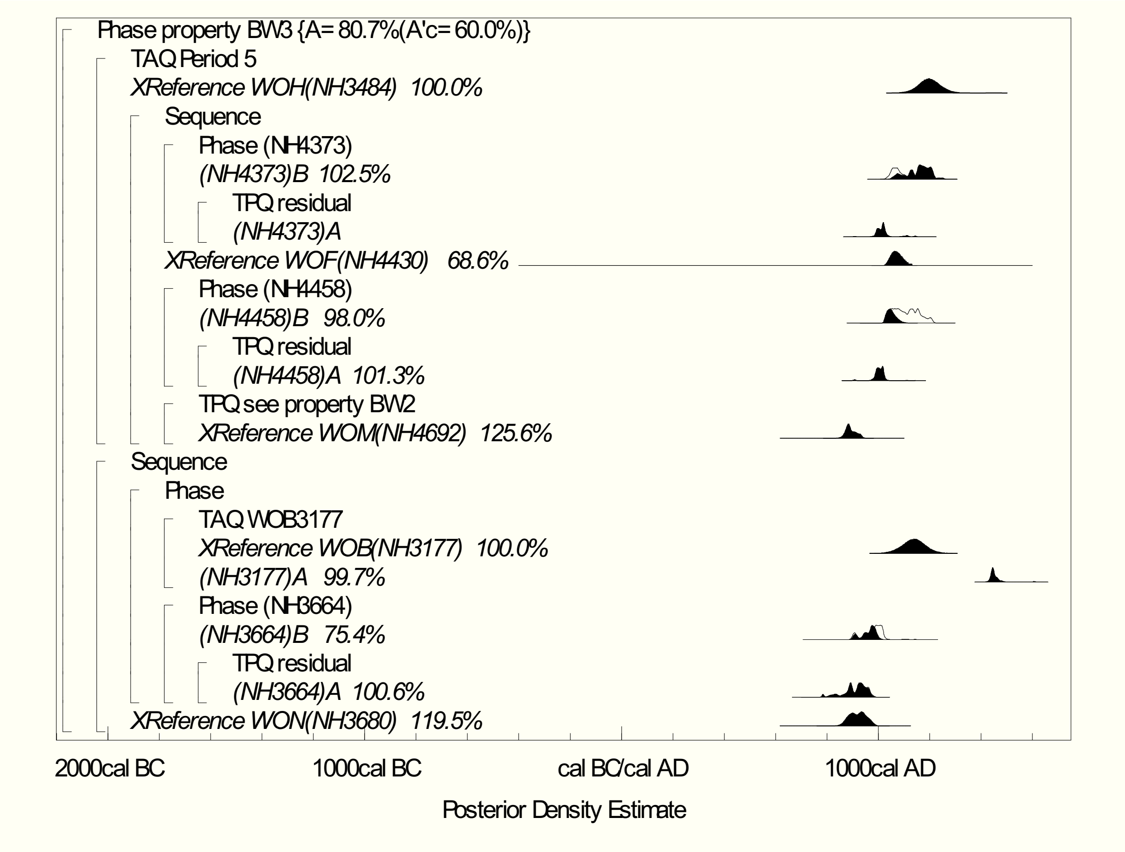

Figure 13: Probability distributions of dates from property BW2 at Northgate House, Winchester. The format is identical to that of **Figure 9**. The large square brackets down the left hand side of **Figures 8–12** along with the OxCal keywords define the overall model exactly.

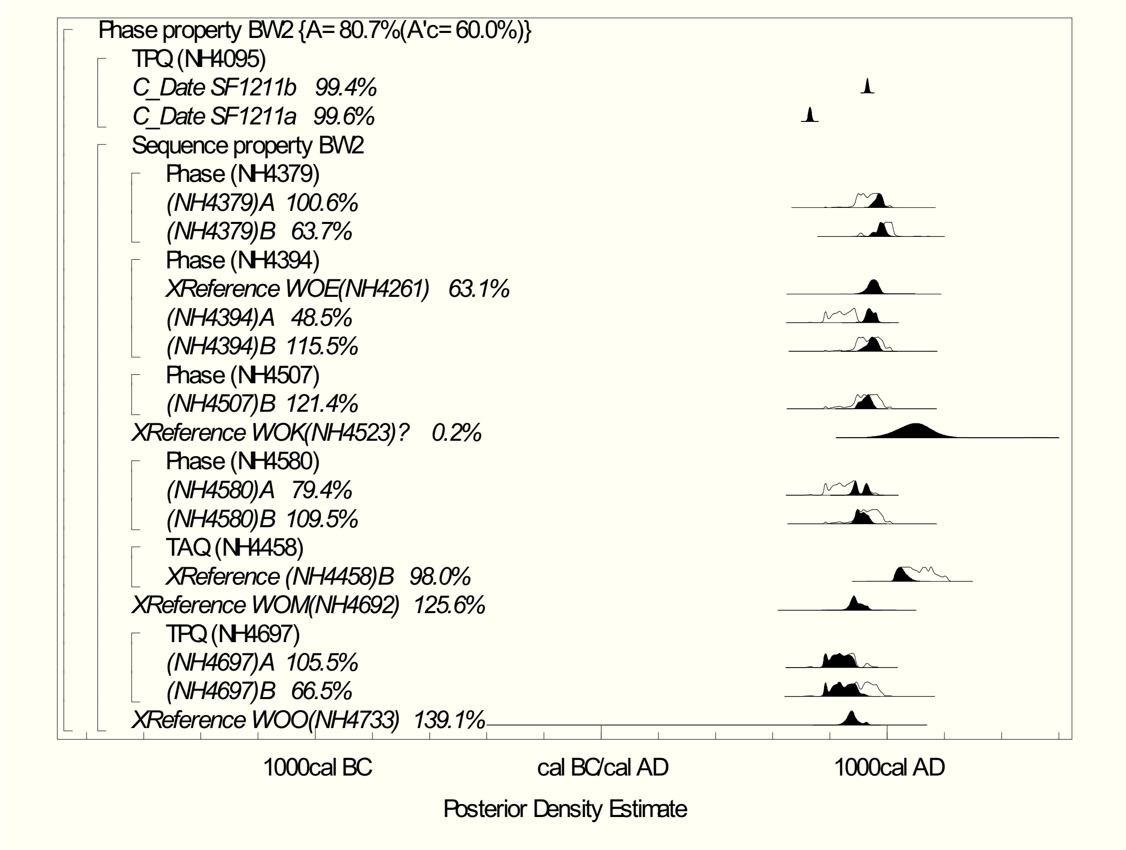

Figure 14: Probability distributions of the first dated events in properties BW2, BW3, BW4, BW5, and BW6 at Northgate House, Winchester, derived from the model defined in **Figures 8- 13**.

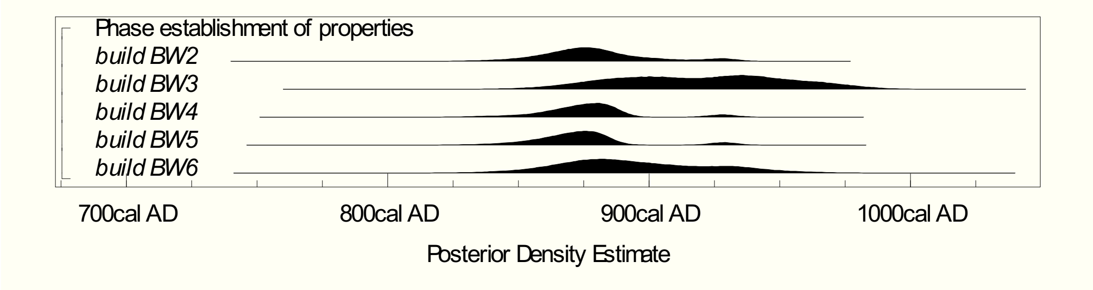

Figure 15: Probability distributions of dates from ceramic phases. Each distribution represents the relative probability that an event occurs at a particular time. Posterior density estimates from the model defined in **Figures 8–12** form the standardised likelihood component of this model. The large square brackets down the left-hand side along with the OxCal keywords define the overall model exactly.

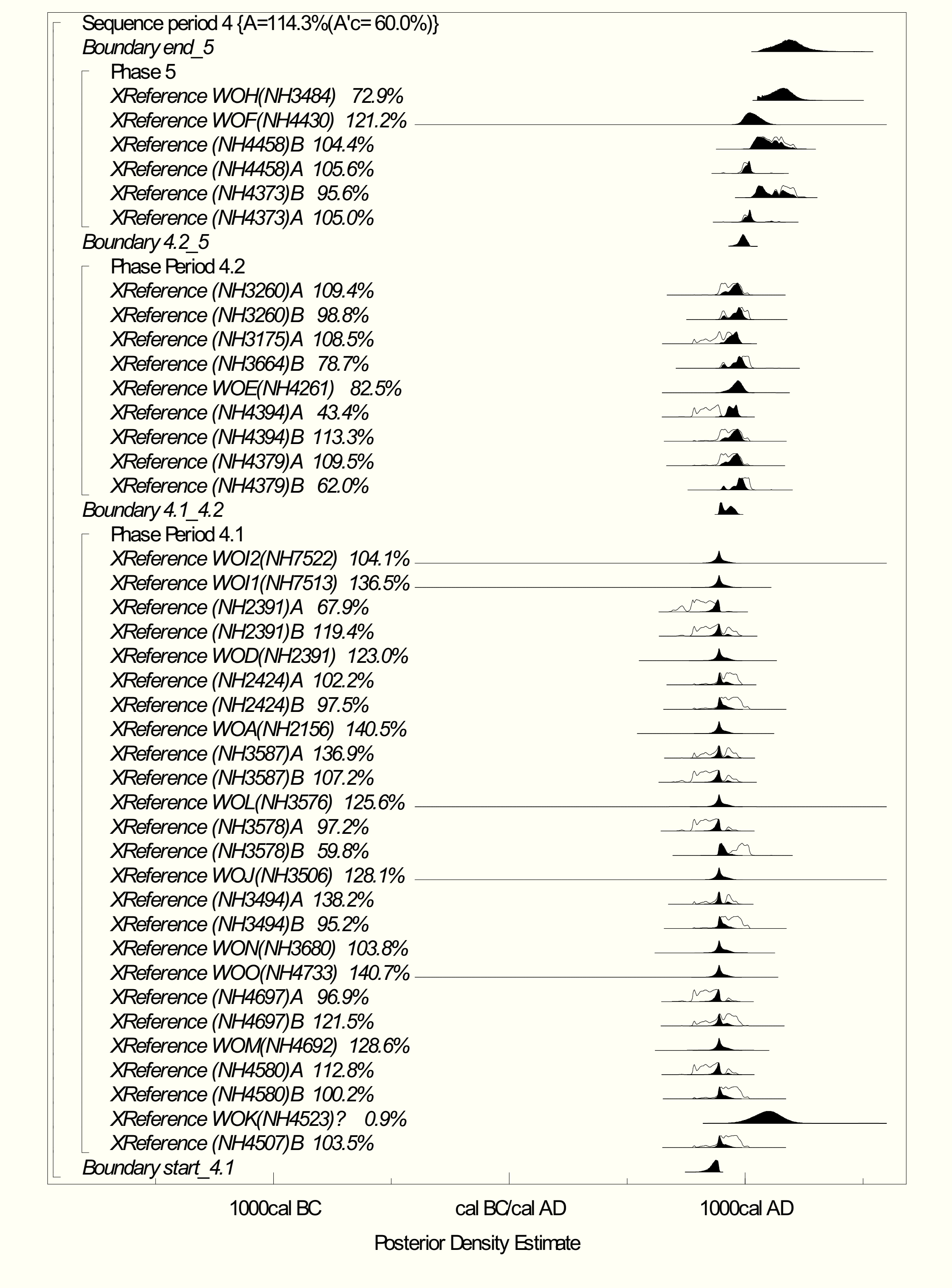

Figure 16: Probability distributions of dates relating to the beginnings and endings of ceramic phases. The distributions are derived from the model shown in Figure 15.

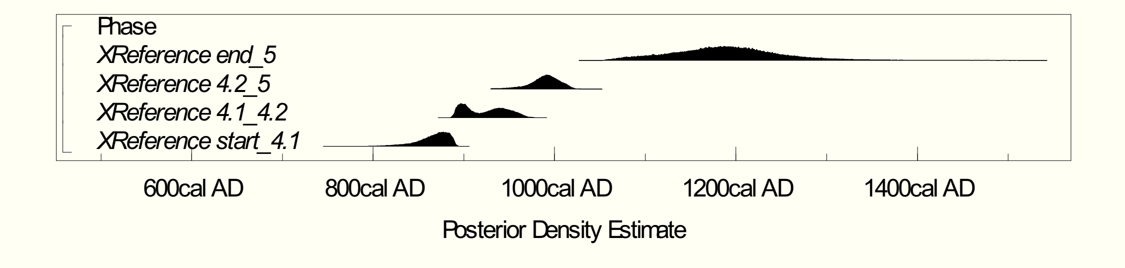

Figure 17: Probability distributions of dates relating to the beginnings and endings of ceramic phases from the alternative model where calibrated radiocarbon dates form the standardised likelihoods component of the model (see text). Each distribution represents the relative probability that an event occurs at a particular time. The large square brackets down the left-hand side along with the OxCal keywords define the overall model exactly.

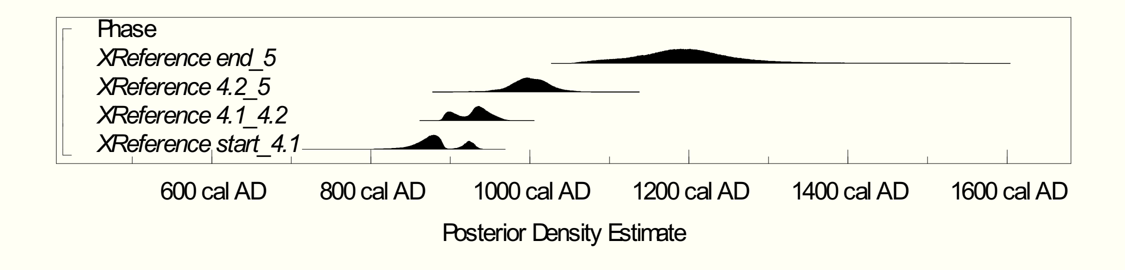

Table 1: List of the hearths sampled for archaeomagnetic dating from Northgate House. N= number of samples per hearth.

	Hearth	Feature No	N	Dimensions
1.	WOA	2156	10	~0.15m thick, 0.6 x 0.45m
2.	WOB	3177	9	~0.10m thick, 1.0 x 1.0m
3.	WOC	5188	8	~0.20m thick, 1.0 x 0.7m
4.	WOD	2391	10	0.02-0.10m thick. Consists of two parts: 0.5 x 1.0m and 1.0 x 1.0m
5.	WOE	4261	8	0.02-0.10m thick, 1.0 x 0.6m
6.	WOF	4430	9	~0.05m thick, 1.0 x 1.3m
7.	WOG	3462	9	~0.03m thick, 3.0 x 0.8m
8.	WOH	3484	8	~0.05m thick. 0.7 x 0.5m
9.	WOI	7513 7511	3 6	~0.04m thick, 0.5 x 0.2m ~0.07m thick, 0.5 x 0.8m
10.	WOJ	3506	8	0.03-0.10m thick, 1.25 x 1.50m
11.	WOK	4523	9	~0.05m thick, 0.25 x 0.80m
12.	WOL	3576	10	~0.05m thick, 1.0 x 1.4m
13.	WOM	4692	9	~0.04m thick, 1.3 x 1.8m
14.	WON	3680	9	0.02-0.05m thick, 0.8 x 1.0m
15.	WOO	4733	9	0.03-0.04m thick, 0.6 x 0.6m
16.	WOP	3780	9	0.03-0.05m thick, 0.3 x 1.2m

Table 2: Radiocarbon determinations from Northgate House, Winchester

Context & Sample Number	Laboratory Number	Material and context	Radiocarbon Age (BP)	$\delta^{13}C$ (‰)	Weighted mean (BP)	Calibrated date range (95% confidence)	*Posterior density estimate (95% probability)*
<234>(NH3587)A	OxA-17173	charcoal, *Betula* sp., from an occupation horizon within property BW4	1153±25	−25.7		cal AD 780-970	*cal AD 830-940*
<234>(NH3587)B	SUERC-13907	charcoal, *Salix/Populus* sp., from the same context as OxA-17173	1175±35	−26.8		cal AD 730-970	*cal AD 830-940*
<232>(NH3578)A	OxA-17172	hazelnut shell from a lens of charcoal associated with the firing of hearth (3576)	1181±27	−26.2		cal AD 770-940	*cal AD 770-900*
<232>(NH3578)B	SUERC-13906	grain, *Triticum* sp., from the same context as OxA-17172	1065±35	−22.9		cal AD 890-1020	*cal AD 890-950*
<225>(NH3494)A	OxA-17181	charcoal, *Corylus* sp., from a occupation layer rich in charred plant remains	1138±24	−25.8	1151±18 (T'=0.7; T'(5%)=3.8 ν=1; Ward and Wilson 1978)	cal AD 780-970	*cal AD 910-970*
<225>(NH3494)A	OxA-17182	replicate of OxA-17182	1166±25	−25.4			
<225>(NH3494)B	SUERC-13917	charcoal, Pomoideae, from the same context as OxA-17181–2	1105±35	−25.9		cal AD 880-1020	*cal AD 900-970*
<174>(NH2391)A	OxA-17137	grain, *Avena* sp., from a layer of *in situ* burning within hearth (2391)	1213±27	−23.0		cal AD 690-890	*cal AD 840-900 (86%)* or *920-950 (9%)*
<174 >(NH2391)B	SUERC-13914	grain, *Avena* sp., from the same context as OxA-17137	1165±35	−25.3		cal AD 770-970	*cal AD 840-950*
<177>(NH2424)A	OxA-17179	charcoal, *Acer* sp., from a layer of charcoal within occupation deposits in property BW4	1130±25	−25.2		cal AD 870-980	*cal AD 880-970*
<177>(NH2424)B	SUERC-13915	charcoal, Pomoideae, from the same context as OxA-17179	1110±35	−27.9		cal AD 880-1020	*cal AD 880-980*
<164>(NH2156)A	OxA-17174	charcoal, Pomoideae, from a layer of *in situ* burning associated with the firing of hearth (2156)	1146±27	−27.3		cal AD 780-980	*cal AD 780-980*
<164>(NH2156)B	SUERC-13908	charcoal, *Salix/Populus*, from the same context as OxA-17174	1030±35	−25.3		cal AD 900-1040	*cal AD 900-1010*
<237>(NH3664)A	OxA-17178	charcoal, *Prunus sp.*, from a layer of *in situ* burning within property	1140±25	−25.0		cal AD 780-980	*cal AD 780-790 (1%)* or *810-980 (94%)*

		BW3					
<237>(NH3664)B	SUERC-13910	charcoal, Pomoideae, from the same context as OxA-17178	1050±35	−26.2		cal AD 900-1030	*cal AD 890-1010*
<211>(NH3177)A	OxA-17175	charcoal, *Prunus spinosa*, from a layer *of in situ* burnt earth within hearth (3177)	432±24	−25.6		cal AD 1430-1470	*cal AD 1420-1490*
<550>(NH4697)A	OxA-17177	charcoal, Pomoideae, from a layer of silting forming over the Saxon street surface, sealed below layers of resurfacing	1181±25	−24.8		cal AD 770-940	*cal AD 770-890*
<550>(NH4697)B	SUERC-13909	charcoal, *Corylus sp*., from the same context as OxA-17177	1140±35	−25.4		cal AD 780-990	*cal AD 770-920*
<289>(NH4580)A	OxA-17183	hazelnut shell from a discrete charcoal-rich deposit associated with *in situ* burning on hearth (4692)	1172±26	−23.1		cal AD 780-960	*cal AD 860-950*
<289>(NH4580)B	SUERC-13918	hazelnut shell from the same context as OxA-17183	1115±35	−22.7		cal AD 830-1010	*cal AD 880-950*
<276>(NH4458)A	OxA-17180	grain, *Triticum* sp., from a discrete area of charred plant remains probably representing rake-out from oven (4485)	1027±25	−21.7		cal AD 980-1030	*cal AD 970-1040*
<276>(NH4458)B	SUERC-13916	grain, *Hordeum* sp., from the same context as OxA-17180	915±35	−25.2		cal AD 1020-1210	*cal AD 1020-1090*
<262>(NH4373)A	OxA-17176	hazelnut shell from an occupation layer above hearth (4430)	1012±25	−24.1		cal AD 990-1030	*cal AD 970-1050 (91%)* or *1090-1120 (4%)*
<262>(NH4373)B	SUERC-13904	grain, *Triticum sp*., from the same context as OxA-17176	885±35	−20.6		cal AD 1030-1220	*cal AD 1050-1230*
<285>(NH4507)B	SUERC-13920	grain, *Avena* sp., from a spread of charred material within an occupation horizon	1120±35	−25.7		cal AD 780-1010	*cal AD 890-960*
<266>(NH4394)A	OxA-17184	charcoal, Pomoideae, from a discrete charcoal spread associated with *in situ* burning on hearth (4261)	1169±26	−27.0		cal AD 780-970	*cal AD 910-980*
<266>(NH4394)B	SUERC-13919	charcoal, *Prunus sp*., from the same context as OxA-17184	1105±35	−25.9		cal AD 880-1020	*cal AD 900-980*
<216>(NH3260)A	SUERC-19280	hazelnut shell, *Corylus avellana*,	1105±30	-20.6		cal AD 880-1020	*cal AD 920-990*

		from occupation horizon (3260)					
<216>(NH3260)B	SUERC-19284	grain, *Avena sativa*, from occupation horizon (3260)	1070±30	-23.9		cal AD 890-1030	*cal AD 930-990*
<208> (NH3175)B	SUERC-19285	grain, *Triticum aestivum*, from occupation horizon (NH3175)	1240±30	-21.0		cal AD 670-890	*cal AD 680-880*
(NH3175)A	SUERC-19286	bone, unfused fragments of sternum, from medium mammal (probably sheep or goat) from occupation horizon (NH3175)	1145±30	-20.1		cal AD 770-990	*cal AD 940-1000*
(NH4379)A	SUERC-19287	bone, cattle rib from occupation horizon (NH4379)	1110±30	-20.9		cal AD 880-1020	*cal AD 930-1000*
(NH4379)B	SUERC-19288	Bone, cattle carpal, articulated with radius from occupation horizon (NH4379)	1040±30	-21.3		cal AD 900-1030	*cal AD 940-1010*
(NH6176)	OxA-16713	Bone, human - right ulna shaft fragment.	1901±28	-18.6		cal. AD 30-210	
(NH6177)A	OxA-16757	Charred bread wheat grain, *Triticum aestivum* from the fill of post-hole (NH6178)	1151±26	-23.4		cal. AD 780-980	
(NH6177)B	OxA-16758	Charred bread wheat grain, *Triticum aestivum* from the fill of post-hole (NH6178)	1134±26	-21.7		cal. AD 820-990	
(NH6204)B	OxA-16759	Charred grain, *Triticum aestivum* from from the fill of pit (NH6203)	1177±26	-23.4		cal. AD 770-950	
(NH6204)A	OxA-16775	Charred grain, *Triticum aestivum* from the fill of pit (NH6203)	1145±55	-20.4		cal. AD 720-1020	
(CC3251)A	OxA-16793	Bone, large mammal cf. cattle - rib from holloway (CC3408)	1966±27	-21		40 cal. BC - cal. AD 90	
(CC3251)B	OxA-16794	Tooth, sheep/goat, from holloway (CC3408)	1669±25	-21.2		cal. AD 260-430	

Table 3: Weighed sample-mean ChRM directions for the hearths from Northgate House, Winchester (φ = 51.065° N, λ = 1.3169° W, SU 47929). Specimen-mean directions for hearth WOI (features 7513 and 7511). Ns= number of data (samples or specimens), K = Fisher concentration parameter. D=declination, I=inclination, α_{95}=95% cone of confidence about the mean direction. Directions variation corrected. The 95% confidence intervals for the Northgate hearths are also shown. For hearth WOI the specimen-averaged directions are used.

	ChRM [°]					**Class**	**Calibrated Date**
Hearth	**D**	**I**	α_{95}	**Ns**	**K**		**(95% confidence)**
WOA	20.4	69.4	3.8	7	252	C	AD 580-AD 1125
WOB	16.6	60.8	2.8	9	333	C	AD 1117-AD 1229
WOC	352.5	66.8	1.9	8	883	A	BC 96-AD 130
WOD	18.7	68.1	2.8	6	584	B	AD 800-AD 1125
WOE	22.7	64.8	3.3	8	269	C	AD 979-AD 1165
WOF	13.7	67.5	2.1	9	625	A	AD 477-AD 1175
WOH	13.6	58.9	2.4	7	652	A	AD 1195-AD 1267
WOI1	20.2	70.8	4.4	19	59	C	AD 559-AD 1084
WOI2	12.9	70.1	3.4	34	52	C	AD 498-AD 1125
WOJ	14.7	67.8	3.9	6	304	C	AD 436-AD 1175
WOK	18.7	62.4	4.3	6	239	B	AD 1065-AD 1245
WOL	13.6	68.1	2.2	8	613	C	AD 498-AD 1148
WOM	22.4	68.9	2.3	6	839	B	AD 880-AD 1093
WON	23.3	67.8	2.9	9	317	A	AD 914-AD 1121
WOO	19.1	69.8	2.5	8	494	A	AD 559-AD 1084
JSB5991	359.2	67.9	2	9	661	??	150BC-AD 130
JSB1572	346.3	66	2.4	11	477	??	96BC-AD 25
SG1-8	30.7	65.9	2.6	6	646	A	AD 975-AD 1102

Table 4: posterior density estimates from alternative models of the dating of the site phases

	Model A (contiguous sequence of posterior density estimates derived from the site chronology)	***Model B (contiguous sequence of dates)***	**Archaeological estimate**
Start site phase 4.1	*cal AD 825-895 (95%)* *cal AD 855-890 (68%)*	*cal AD 825-895 (74%) or 905-940 (21%)* *cal AD 855-895 (58%) or 915-930 (10%)*	850 AD
Transition site phase 4.1-4.2	*cal AD 855-965 (95%)* *cal AD 890-910 (34%) or 925-955 (34%)*	*cal AD 890-965 (95%)* *cal AD 890-910 (17%) or 925-955 (51%)*	950 AD
Transition site phase 4.2-5	*950-1020 (95%)* *cal AD 975-1010 (68%)*	*cal AD 945-1055 (95%)* *cal AD 975-1025 (68%)*	1050 AD
End site phase 5	*cal AD 1060-1305 (95%)* *cal AD 1125-1245 (68%)*	*cal AD 1065-1325 (95%)* *cal AD 1130-1250 (68%)*	1225 AD

WINCHESTER
A CITY IN THE MAKING

Archaeological excavations between 2002 – 2007
on the sites of Northgate House, Staple Gardens and the former Winchester Library, Jewry St

This is one of the
19 specialist reports
provided with
the above publication

Oxford Archaeology
Monograph

ISBN 978-0-904220-62-9

oxfordarchaeology
southsouthsouth